Developmental Biology 443 (2018) 188–202

Contents lists available at ScienceDirect

Developmental Biology

journal homepage: www.elsevier.com/locate/developmentalbiology

A mosaic of independent innovations involving *eyes shut* are critical for the evolutionary transition from fused to open rhabdoms

Simpla Mahato[a], Jing Nie[a,1], David C. Plachetzki[b,*], Andrew C. Zelhof[a,*]

[a] Department of Biology, Indiana University, Bloomington, IN 47405, USA
[b] Molecular, Cellular, and Biomedical Sciences, University of New Hampshire, Durham, NH 03824, USA

ABSTRACT

A fundamental question in evolutionary biology is how developmental processes are modified to produce morphological innovations while abiding by functional constraints. Here we address this question by investigating the cellular mechanism responsible for the transition between fused and open rhabdoms in ommatidia of apposition compound eyes; a critical step required for the development of visual systems based on neural superposition. Utilizing *Drosophila* and *Tribolium* as representatives of fused and open rhabdom morphology in holometabolous insects respectively, we identified three changes required for this innovation to occur. First, the expression pattern of the extracellular matrix protein Eyes Shut (EYS) was co-opted and expanded from mechanosensory neurons to photoreceptor cells in taxa with open rhabdoms. Second, EYS homologs obtained a novel extension of the amino terminus leading to the internalization of a cleaved signal sequence. This amino terminus extension does not interfere with cleavage or function in mechanosensory neurons, but it does permit specific targeting of the EYS protein to the apical photoreceptor membrane. Finally, a specific interaction evolved between EYS and a subset of Prominin homologs that is required for the development of open, but not fused, rhabdoms. Together, our findings portray a case study wherein the evolution of a set of molecular novelties has precipitated the origin of an adaptive photoreceptor cell arrangement.

1. Introduction

Compound eyes are common visual structures found in a wide range of arthropods (Land and Nilsson, 2002). Within compound eyes, the ommatidium is the fundamental repeated modular unit required for the detection of light. An ommatidium contains photoreceptor neurons and each photoreceptor has a light gathering organelle known as the rhabdomere. The rhabdom is the collection of all rhabdomeres within a single ommatidium. Rhabdoms may be arranged in two configurations: open rhabdoms have a pronounced inter-rhabdomeral space (IRS) while fused rhabdoms lack the IRS.

The majority of insects have fused rhabdoms but open rhabdoms are thought to have evolved in both crustacean and insect lineages at least five times independently (reviewed in Osorio, 2007). The evolutionary origins of open rhabdoms is also tightly associated with the origins of neural superposition architecture where photoreceptor neural projections from the rhabdoms of adjacent ommatidia are pooled within the lamina, thus amplifying signal by allowing neurally encoded light information from multiple ommatidia to reach the same laminar neurons. Neural superposition stands in contrast to apposition eye architecture where light information from a single ommatidium is kept discrete (Land and Horwood, 2005 and reviewed in Osorio, 2007). Like fused rhabdoms, apposition eyes are the condition of most insects, and crustaceans (Osorio, 2007).

The higher order Diptera of the suborder Brachycera (including houseflies, horse flies and fruit flies) contain open rhabdoms and neural superposition architecture. This configuration enables an increase in light sensitivity without a commensurate loss of visual acuity (Agi et al., 2014; Braitenberg, 1967; Kirschfeld, 1967). Interestingly, even though open rhabdoms have evolved independently several times, there are no known examples of loss of the open rhabdom among Brachycera (Osorio, 2007), which are known for their fast flying capabilities (Friedrich, 2010). In addition, some non-brachyceran dipterans also possess open rhabdoms. Species of the mosquito genus *Toxorhynchites* (suborder Nematocera) also possess an open rhabdom and neural superposition (Land et al., 1999; Land and Horwood, 2005). In contrast to other mosquitos, *Toxorhynchites* is diurnal, large, and has swift flight abilities (Land and Horwood, 2005) suggesting a

* Corresponding authors.
E-mail addresses: David.Plachetzki@unh.edu (D.C. Plachetzki), azelhof@indiana.edu (A.C. Zelhof).
[1] Current address: Department of Otolaryngology-Head and Neck Surgery, Indiana University School of Medicine, Indianapolis, IN 46202, USA.

https://doi.org/10.1016/j.ydbio.2018.09.016
Received 19 June 2018; Received in revised form 18 September 2018; Accepted 18 September 2018
Available online 19 September 2018

fitness advantage for open rhabdoms related to higher visual acuity in insects with high performance flight.

The genetic and molecular dissection of *Drosophila* open rhabdoms has begun to unravel the developmental mechanisms required for this adaptation in holometabolous insects. Genetic screens identified two key proteins, Eyes Shut (EYS; a.k.a. Spacemaker) and Prominin, that are central to the development of the open rhabdom (Husain et al., 2006; Zelhof et al., 2006). EYS and Prominin are elements of a cellular network that generates the IRS involving the secretion of an extracellular matrix, steric hindrance of adhesion and cellular contraction (Gurudev et al., 2014; Husain et al., 2006; Nie et al., 2012, 2014; Zelhof et al., 2006). EYS and Prominin are not restricted to open rhabdom species such as *Drosophila* but are instead widely conserved among insects, including species with fused configurations (Husain et al., 2006; Zelhof et al., 2006). However, the differences in the structure and function of EYS and Prominin that underpin these alternative ommatidial morphologies remain unclear.

Here we explore this question by combining functional analyses of EYS and Prominin orthologs from *Drosophila* and *Tribolium,* representatives of the open and fused rhabdom systems of holometabolous insects respectively, with comparative phylogenetic analyses of these loci from selected holometabolous insects. Our findings show that the morphological transformation from a fused to an open rhabdom in *Drosophila* was based on a mosaic of innovations including: 1) the co-option of rhabdomeric photoreceptor expression from mechanosensory neurons, 2) a change in protein structure of EYS that permitted the targeting of EYS to the apical membrane of photoreceptors, without ablating its function in mechanosensory neurons, and 3) the origination of a novel interaction between EYS and Prominin that facilitated the expansion of the IRS. Moreover, comparative phylogenetic analyses suggest that these molecular innovations may be common among holometabolous insect species with open rhabdoms. Together, our findings depict a set of cellular and molecular innovations required for the adaptive transition from fused to open rhabdoms in holometabolous insect compound eye development.

2. Materials and methods

2.1. Species tree estimation

We selected 17 high-quality genome and transcriptome datasets from species representing the major lineages of holometabolous insects where ommatidial morphology was known, including representative brachycerid and nematocerid dipterans. We constructed a set of orthologs for phylogenomic analysis using the partitions described in (Misof et al., 2014) and our custom reciprocal BLAST scripts. Briefly, our procedure first extracted the sequence data from each partition for the reference species *Drosophila melanogaster* and BLASTed that sequence back against the dmel-R6 protein set (Gramates et al., 2017). The resulting top hit was in turn BLASTed against each of our 16 species protein model datasets. Resulting best hits were then blasted back against the dmel-R6 protein set and each sequence for which both the original and secondary blast searches hit the same protein in the dmel-R6 protein set was retained as a representative ortholog for that species. Individual partitions that had greater than 90% taxon occupancy were aligned using MAFTT (Katoh and Standley, 2016) under default parameters, trimmed using the gblocks_wrapper.pl and concatenated using custom scripts. The resulting phylogenomic dataset included 37 partitions and had a total length of 16,976 amino acid positions. Phylogenetic reconstruction was done using Phylobayes MPI under the CAT+GTR+Γ (Rodrigue and Lartillot, 2014).

2.2. Ancestral state reconstruction

For ancestral state reconstruction, we encoded each species as having either a fused or an open rhabdom. We then reconstructed the ancestry of the fused/open character state using make.simmap implemented in the R package phytools (https://doi.org/10.1111/j.2041-210X.2011.00169.x). Character state transitions were modeled under equal rates and 10,000 simulated histories were examined.

2.3. Gene tree estimation

The same protein sets used for phylogenetic reconstruction were also used for EYS and Prominin gene tree estimation, with the exception that sequences from vertebrate model taxa were also included. Here, BLAST (Altschul et al., 1990) searches using EYS (AAZ83988.3) and Prominin (NP_001286843.1), both from D. melanogaster, were conducted and the top 10 hits above an e-value of 0.001 were retained. Sequences were aligned using MAFFT under default parameters and phylogenies were estimated using RaXML under the AUTO model setting. Initial phylogenies for both EYS and Prominin included several clades of closely related paralogs (data not shown). From these large gene family trees, we then pruned the focal EYS or Prominin clades from these trees and realigned these sequences in MAFTT under default parameters. Phylogenetic estimation was then done using RaXML (Stamatakis, 2014) with 20 random starts under the AUTO model setting. We also conducted 1000 bootstrap replicates and support was assessed by mapping bootstrap replicates onto the best scoring tree from the previous step. All data and scripts used in the phylogenetic aspects of the study are available at https://github.com/plachetzki/EYS_PROM.

2.4. Drosophila stocks and cDNAs

All crosses and staging were performed at 23 °C. *Drosophila* stocks used in this study include: UAS-Dm-*eys*, UAS-Dm-*prominin*, *prom*^{1}, *eys*^{1} (Zelhof et al., 2006), prom-gal4 (Nie et al., 2012). chp-gal4 (BDSC#47686), elav-gal4 (BDSC #458), UAS-mCD8-GFP (BDSC #5137), Dm-EYS-GFP 1 (BDSC # 63162) were obtained from the Bloomington Drosophila Stock Center. The following stocks were created for this study UASattB- Dm5′Tc-*eys*, UASattB-Tc5′Dm-*eys*, UASattB-Tc-*eys*, UASattB-Tc-*prominin-like,* UASattB-Dm *GFP-eys* and inserted into y-attP-3B (BDSC#24871), UAS-Dm EYS-GFP 2 and UAS-Dm-*prominin-like*. A full-length cDNA representing *Tribolium eys* was generated from RT-PCR reactions (SuperScript III First Strand Synthesis, Invitrogen) from total RNA isolated from *Tribolium* v^{W} stock, respectively. cDNA representing isoform *Drosophila prominin-like B* was obtained from the Drosophila Genomics Resource Center (DGRC # 130400). The 5′ ends of *Musca domestica* and *Toxorhynchites amboinensis eys* were confirmed by 5′RACE (Generacer Core Kit, Invitrogen). *Musca domestica* were obtained from Carolina Biologicals (Item #144410) and mRNA and total RNA for *Toxorhynchites amboinensis* was obtained from Dr. J. Pitts (Baylor University). Chimeric cDNAs were produced utilizing NEBuilder HiFi assembly (New England Biolabs).

2.5. Antibody production

Tribolium EYS antibody production: The first 310 amino acids of the ORF was fused to GST and used as an antigen in rats (Cocalico Biologicals). *Drosophila* Prominin-like antibody production: – The C-terminal peptide SERDREHVPLANVPKK (produced in the laboratory of Dr. Charles Zuker) was used as the antigen in rabbits.

2.6. Transmission electron microscopy, immunofluorescence staining, and imaging

Drosophila eye samples were prepared for transmission electron microscopy (TEM) as previously described (Nie et al., 2015). All crosses were maintained at 23 °C and adult heads were fixed within 8 h after eclosion. Pupal retinas were staged at 23 °C, dissected in PBS,

and fixed in PBS containing 4% formaldehyde for 10 min. *Drosophila* embryos were collected and fixed as described in Zelhof et al. (2001). *Tribolium* embryos were collected and fixed as described in Brown et al. (2009) but late stage embryos were selected and manually dechorionated before incubation with primary antibody. The primary antibodies used were: mouse anti-EYS (mAb 21A6, 1:50, Developmental Studies Hybridoma Bank); rabbit anti-Prom (1:100) (Zelhof et al., 2006); rat anti-Tc-EYS (1:50), Rhodamine (1:200) or Alexa Fluor 647 (1:50) conjugated phalloidin (ThermoFisher Scientific) was used for the detection of F-actin. The FITC or RX secondary antibodies (1:200) were obtained from Jackson ImmunoResearch Laboratories. Confocal images were taken on a Leica TCS SP5 and TEM was performed with a JOEL 1010 and all images were processed in Adobe Photoshop.

2.7. Rhabdom morphology

The following references contained descriptions that were utilized to determine whether the species analyzed contained an open or fused rhabdom: *Bombus hortorum* (Meyer-Rochow, 1981), *Apis mellifera* (Zelhof et al., 2006), *Tribolium castaneum* (Zelhof et al., 2006), *Heliconius erato* (McCulloch et al., 2016), *Danaus plexippus* (Sauman et al., 2005), *Plutella xylostella* (Wang and Hsu, 1982), *Bombyx mori* (Eguchi et al., 1962), *Drosophila melanogaster* (Zelhof et al., 2006), *Musca domestica* (Zelhof et al., 2006), *Bractrocera dorsalis* (Liu et al., 2017), *Anophele gambiae* (Zelhof et al., 2006), *Culex quinquefasciatus* (unpublished data), *Toxorhynchites brevipalpis* (Land et al., 1999; Zelhof et al., 2006), Aedes aegypti (Brammer, 1970).

2.8. Cell transfections, co-immunoprecipitations and westerns

Cell transfection assays and immunofluorescence were performed as previously described (Nie et al., 2012; Zelhof et al., 2006) utilizing Qiagen Effectene. S2 DGRC cells were obtained from the Drosophila Genomics Resource Center (DGRC #6). A GFP nanobody (Allele) was used to immunoprecipitate GFP containing proteins from S2 cell extracts according to the manufacture instructions. Proteins were separated on Mini-Protean TGX gels (BIO-RAD) and transferred to Immobilon membranes (Millipore). Antibodies utilized were rabbit anti-GFP (ab290-Abcam) and mouse monoclonal anti-alpha Tubulin (T9026-Sigma). Signal detection was achieved with use of a HRP-conjugated anti-mouse or anti-rabbit secondary antibody (1:5000) (Jackson ImmunoResearch Laboratories) combined with Superscript West Pico Chemiluminescent Substrate (Thermo Scientific).

2.9. Signal sequence and transmembrane domain analyses

The following programs were utilized to analyze protein structures: SignalP 4.1 Server, HMMER, and TMHMM Server v. 2.0.

KEY RESOURCES TABLE

Reagent or resource	Source	Identifier
Antibodies		
Rat anti-Tribolium EYS	This Paper	N/A
Rabbit anti-Drosophila Prominin-like	This Paper	N/A
21A6 Mouse monoclonal anti-Drosophila EYS	Developmental Studies Hybridoma Bank	AB 528449
Rabbit anti-Drosophila Prominin	Zelhof et al. (2006)	N/A
Rabbit anti-GFP	Abcam	ab290
Mouse monoclonal anti-alpha Tubulin	Sigma	T9026
HRP-conjugated anti-mouse	Jackson ImmunoResearch Laboratories	715-035-150
HRP-conjugated anti-rabbit	Jackson ImmunoResearch Laboratories	111-035-144
Rhodamine conjugated phalloidin	ThermoFisher Scientific	R415
Alexa Fluor 647 conjugated phalloidin	ThermoFisher Scientific	A22287
FITC or RX conjugated secondary antibodies Against Rat, Rabbit, and Mouse	Jackson ImmunoResearch Laboratories	
GFP-nano antibody	Allele Biotechnologies	
Bacterial and Virus Strains		
Biological Samples		
Chemicals, Peptides, and Recombinant Proteins		
Critical Commercial Assays		
Deposited Data		
Sequences	This paper	https://github.com/plachetzki/EYS_PROM
Experimental Models: Cell Lines		
Drosophila S2 DGRC cell line	Drosophila Genomics Resource Center	DGRC #6
Experimental Models: Organisms/Strains		
UAS-Dm-*eys*	Zelhof et al. (2006)	
UAS-Dm-*prominin*	Zelhof et al. (2006)	
prom^{1}	Zelhof et al. (2006)	
eys^{1}	Zelhof et al. (2006)	
prom-gal4	Nie et al. (2012)	
chp-gal4	Bloomington Drosophila Stock Center	BDSC#47686
elav-gal4	Bloomington Drosophila Stock Center	BDSC #458
UAS-*mCD8-GFP*	Bloomington Drosophila Stock Center	BDSC #5137
Dm-EYS-GFP 1	Bloomington Drosophila Stock Center	Dm-EYS-GFP 1
UASattB- Dm5′Tc-*eys*	This Paper	
UASattB-Tc5′Dm-*eys*	This Paper	
UASattB-Tc-*eys*	This Paper	
UASattB-Tc-*prominin-like*	This Paper	
UASattB-Dm *GFP-eys*		BDSC#24871
y-attP-3B	Bloomington Drosophila Stock Center	
UAS-Dm EYS-GFP 2	This Paper	
UAS-Dm-*prominin-like*	This Paper	

Musca domestica	Carolina Biologicals	Item #144410
Oligonucleotides		
Recombinant DNA		
isoform *Drosophila prominin-like B* cDNA	Drosophila Genomics Resource Center	DGRC # 130400
Software and Algorithms		
SignalP 4.1 Server	http://www.cbs.dtu.dk/services/SignalP/	
HMMER	http://hmmer.org/	
TMHMM Server v. 2.0	http://www.cbs.dtu.dk/services/TMHMM/	
RaXML	Stamatakis et al. (2014)	https://github.com/stamatak/standard-RAxML
MAFFT	Katoh and Standley (2016)	https://github.com/smirarab/pasta
Custom scripts	This paper	https://github.com/plachetzki/EYS_PROM

3. Results

3.1. The ancestral holometabolous insect possessed a fused rhabdom

Our phylogenetic analyses focused on a selection of phylogenetically informative holometabolous insect species that that represent both fused and open rhabdom configurations. Phylogenomic tree estimation resulted in a well-resolved species tree with maximum support (posterior probability) for each node. Our tree is in agreement with recent phylogenetic analyses of insect phylogeny (Misof et al., 2014). We analyzed the evolutionary history of rhabdom configuration among our selected holometabolous insect taxa using ancestral state reconstruction. Our analyses provide strong support ($P = 1.0$) for the hypothesis that the last common ancestor of holometabolous insects had a fused rhabdom and that transitions of this morphology to the open configuration likely occurred within Diptera on multiple occasions; once along the branch leading to Brachycera and once, within the Nematocera along the branch leading to *Toxorhynchites*. Therefore, the open rhabdom morphologies of *Drosophila* and *Toxorhynchites* represent evolutionary innovations (Fig. 1).

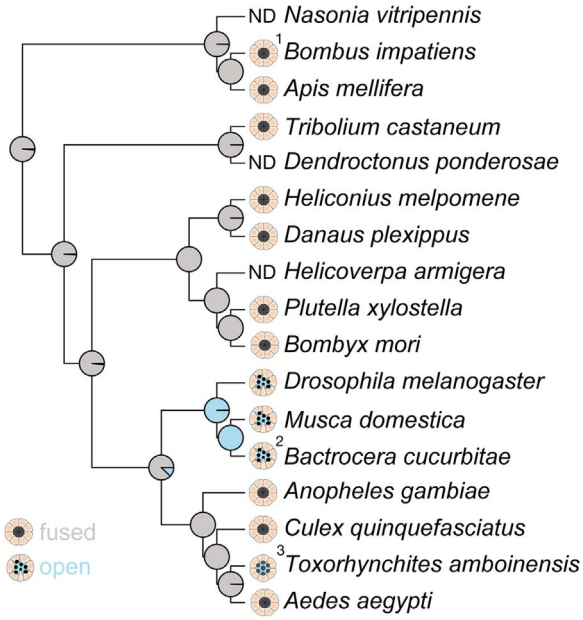

Fig. 1. The ancestral holometabolous insect possessed a fused rhabdom. Studies of character evolution using Bayesian simulation mapping show that open rhabdoms have evolved from a fused state at least twice in the history of holometabolous insects. The ommatidial arrangement of each taxon is shown. Pie graphs at nodes indicate the posterior probability of reconstructed ancestral states. ND – not determined. [1]The rhabdom structure was determined for *Bombus hortorum*. [2]The rhabdom structure was determined for *Bactrocera dorsalis*. [3]The rhabdom structure was determined for *Toxorhynchites brevipalpis* and the rhabdom is open but not trapezoidal.

3.2. Homologous rescue of eys mutant phenotypes is dependent upon sensory cell context

Previous data have demonstrated that *Drosophila eys* is expressed in the photoreceptors of open rhabdoms and the loss of *Drosophila* EYS (Dm-EYS) resulted in a fused arrangement of the rhabdomeres (Husain et al., 2006; Zelhof et al., 2006) (Fig. 2A, B). We tested the functional equivalence of Dm-EYS and *Tribolium* EYS (Tc-EYS) by assaying their ability to rescue photoreceptor rhabdom arrangement and mechanosensory neuron function in *Drosophila eys* mutants (Cook et al., 2008; Husain et al., 2006; Zelhof et al., 2006). In *Drosophila*, EYS constitutes part of the extracellular matrix of the IRS that separates each individual rhabdomere within an ommatidium. No rescue of the photoreceptor phenotype was noted upon expression of Tc-EYS in photoreceptors of *Drosophila eys* mutants, in contrast to experiments with Dm-EYS (Fig. 2C, D). In Tc-EYS rescue experiments we observed a fused rhabdom and only very limited separation of the photoreceptor stalk membranes juxtaposed to the adherens junctions of photoreceptor cells. In mechanosensory neurons, EYS functions as a protective barrier that safeguards cell shape under environmental stress, heat and changes in osmolarity; *eys* mutants become increasingly discoordinated when exposed to high temperatures and this behavior is directly correlated to the loss of mechanosensory function (Cook et al., 2008). When Tc-EYS is expressed in *Drosophila eys* mutant mechanosensory organs with a pan-neuronal driver, Elav-Gal4, we found that Tc-EYS was capable of rescuing the mutant mechanosensory defect (Fig. 3), such that the flies were resistant to heat induced discoordination. These results suggest that functional equivalency is dependent upon cellular context; Tc-EYS is apparently functional in *Drosophila* mechanosensory neurons but not in rhabdomeric photoreceptors.

3.3. Tc-EYS functional rescue is dependent on spatial localization

We examined the localization of Tc-EYS in both photoreceptor and mechanoreceptor cell types in order to understand the basis for our observation that Tc-EYS could rescue mechanoreceptor, but not photoreceptor, deficiencies in *Drosophila eys* mutants. In photoreceptors, Tc-EYS was detected only in cell bodies, but not at the apical photoreceptor membrane as is Dm-EYS during the critical period of IRS formation (Fig. 4A–C). In contrast, in mechanosensory neurons, Tc-EYS localization was identical to that of Dm-EYS (Fig. 5A–C). Here, Tc-EYS accumulation was observed at the cavity interface, the junction of the apical surface of the sensory neuron with the lymph space, and inside the lymph space juxtaposed to the ciliary dilation. Thus, the differential ability of Tc-EYS to rescue *eys* mutants appears to be dependent on its correct intracellular localization in the respective sensory neuron.

The ability of Tc-EYS to localize and function in both *Tribolium* and *Drosophila* mechanosensory neurons suggests that EYS was co-opted for a novel function in photoreceptors with open configurations. Therefore, we expected to observe Tc-EYS expression in mechanosensory organs of *Tribolium* but not in the retina as suggested by our previous analysis of Tc-EYS mRNA expression (Zelhof et al., 2006). Utilizing our Tc-EYS antibody we find that Tc-EYS is expressed in many neuronal cell types of the *Tribolium* embryonic peripheral

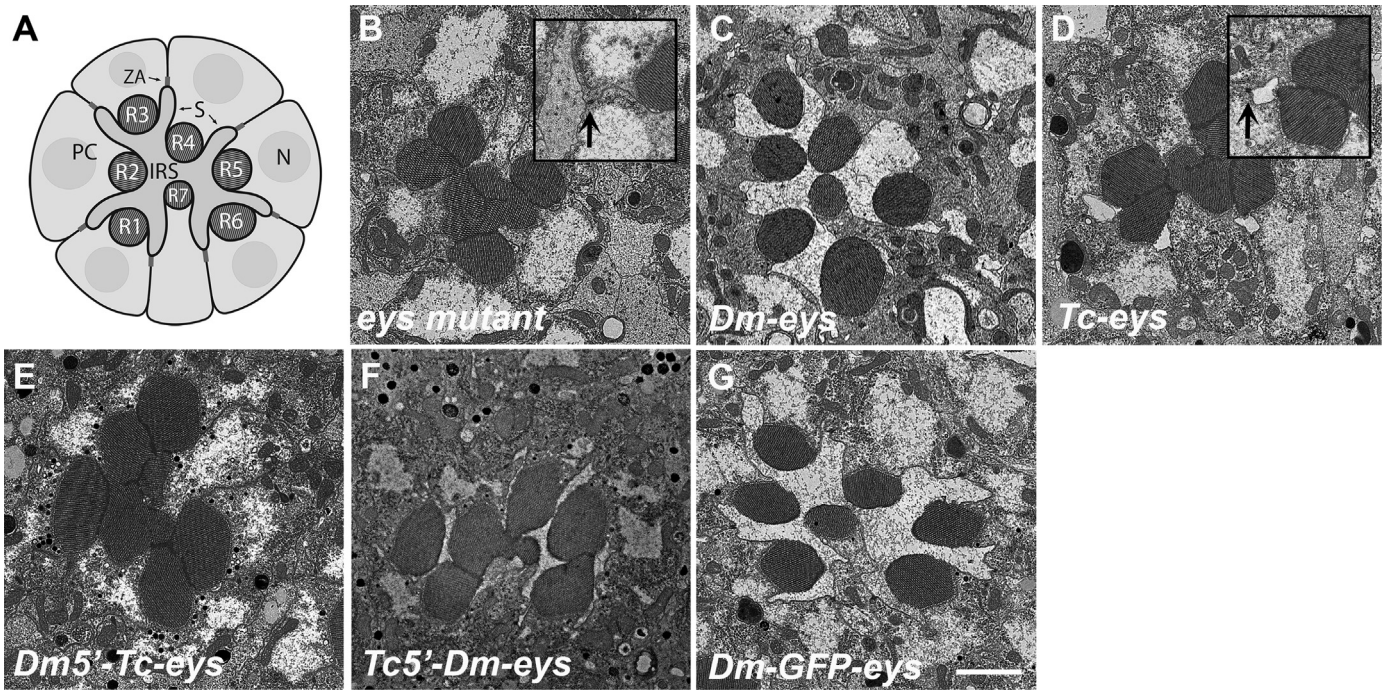

Fig. 2. *Drosophila* EYS and *Tribolium* EYS homologs are not functionally equivalent in photoreceptors. Transmission electron micrographs of adult *Drosophila* ommatidium. A) Schematic of wild type, B) *eys* mutant, C) *eys*, Dm-*eys* rescue, D) *eys*, Tc-*eys* rescue, E) *eys*, Dm5′Tc-*eys* rescue, F) *eys*, Tc5′Dm-*eys* rescue, G) *eys*, Dm-GFP-*eys* rescue. Arrows indicate adherens junctions between photoreceptors. IRS – inter-rhabdomeral space. S – stalk membrane. ZA – zonula adherens. PC – photoreceptor cell. N – nucleus. Scale Bar 2 µm. Genotypes: B) *w; eys^1/eys^1*, C) *w; eys^1/eys^1; uas Dm-eys/chp-gal4*, D) w; eys^1/eys^1; uas Tc-eys/chp-gal4, E) *w; eys^1/eys^1; uas Dm5′Tc-eys/chp-gal4*, F) *w; eys^1/eys^1; uas Tc5′ Dm-eys/chp-gal4*, G) *w; eys^1/eys^1; uas Dm-GFP-eys/chp-gal4*.

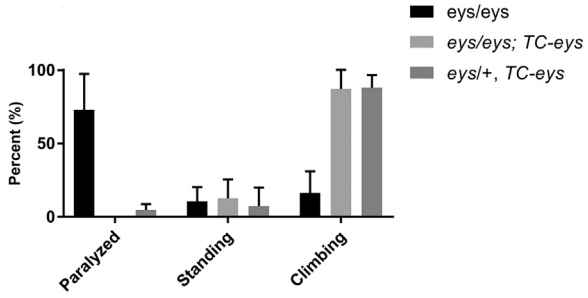

Fig. 3. The *Tribolium* EYS homolog can rescue *eys* deficient ciliary mechanoreceptor neurons. Expression of Tc-EYS in *Drosophila* neurons (ELAV-GAL4) rescues mechanosensory defects associated with *eys* mutants. Four separate trials of each genotype were conducted. Males and females were heat-shocked for 1 h at 37 °C, allowed to recover for 15 min, and then each vial was mechanically agitated twice and allowed to recover for five minutes. The animals were scored for the following characteristics: *paralyzed* – on back or side on the floor of vial, *standing* – upright on floor of vial, *climbing* – on the side of the vial. Numbers of animals in each category were calculated for each genotype.

nervous system (Fig. 5G). In particular, we observed a repetitive pattern in each of the abdominal segments resembling the lateral pentascolopidial chordotonal organs of *Drosophila*. Moreover, cellular localization of Tc-EYS in these cells is highly reminiscent of a similar developmental stage in *Drosophila* embryos (Fig. 5E–H). Tc-EYS expression was not detected in *Tribolium* photoreceptors during photoreceptor morphogenesis (data not shown). Together, these results suggest that the transition from a fused to open rhabdom requires an expanded expression pattern of EYS to photoreceptors.

3.4. A novel amino terminus extension is sufficient for EYS localization to the apical photoreceptor membrane

Whereas presently unknown regulatory changes are implicated in the expanded expression pattern of EYS to photoreceptors, these changes cannot fully account for the adaptation of fused to open rhabdoms because Tc-EYS does not rescue *eys* mutants when expressed in *Drosophila* photoreceptors. Therefore, we reexamined the various structural features of both EYS homologs to determine potential differences that could account for the lack of functional equivalency in photoreceptors. Both Dm-EYS and Tc-EYS contained the same number and arrangement of EGF and Laminin G repeats (Fig. 6). Furthermore, as expected for a secreted protein, Tc-EYS contained a typical signal sequence, on the N-terminus just prior to the first EGF domain. In contrast, the N-terminus of Dm-EYS begins with a large stretch of amino acids that appears to internalize the signal sequence, which is also located just before the first EGF repeat (Fig. 6). This novel extension of the N-terminus correlated with dipteran species with open rhabdoms (Fig. 7). To further explore this, we aligned the predicted EYS sequences from 17 species of *Drosophila* with additional EYS sequences from other brachyceran and nematoceran speices (data not shown). This analysis revealed several conserved motifs in the amino terminus of *Drosophila* speices, but several apparent indels were also present among *Drosophila* EYS sequences. The *Drosophila* amino terminus sequence showed very little similarity to the EYS sequences of other brachyceran species and even less similarity with the nematoceryan EYS sequences, including *Toxorhynchites*.

To test if this structural variation is necessary and sufficient for EYS function in rhabdomeric photoreceptors, we generated two chimera proteins in which the amino terminus of Tc-EYS and Dm-EYS prior to the first EGF domain were exchanged (Dm5′Tc-EYS and Tc5′Dm-EYS – Fig. 6) and tested for function in *Drosophila* photoreceptors. Exchanging the first 30 amino acids of Tc-EYS with the first 147 amino acids of Dm-EYS, prior to the first EGF repeat, resulted in the redirection of Tc-EYS to the photoreceptor apical region during the initial period of IRS formation in wild type photoreceptors (Fig. 4F). However, we did not observe any accumulation of the chimera protein in the IRS 24 h later (data not shown) and the chimera protein was not capable of rescuing of the *eys* mutant phenotype (Fig. 2E). When the amino terminus of *Drosophila* EYS was replaced with the amino

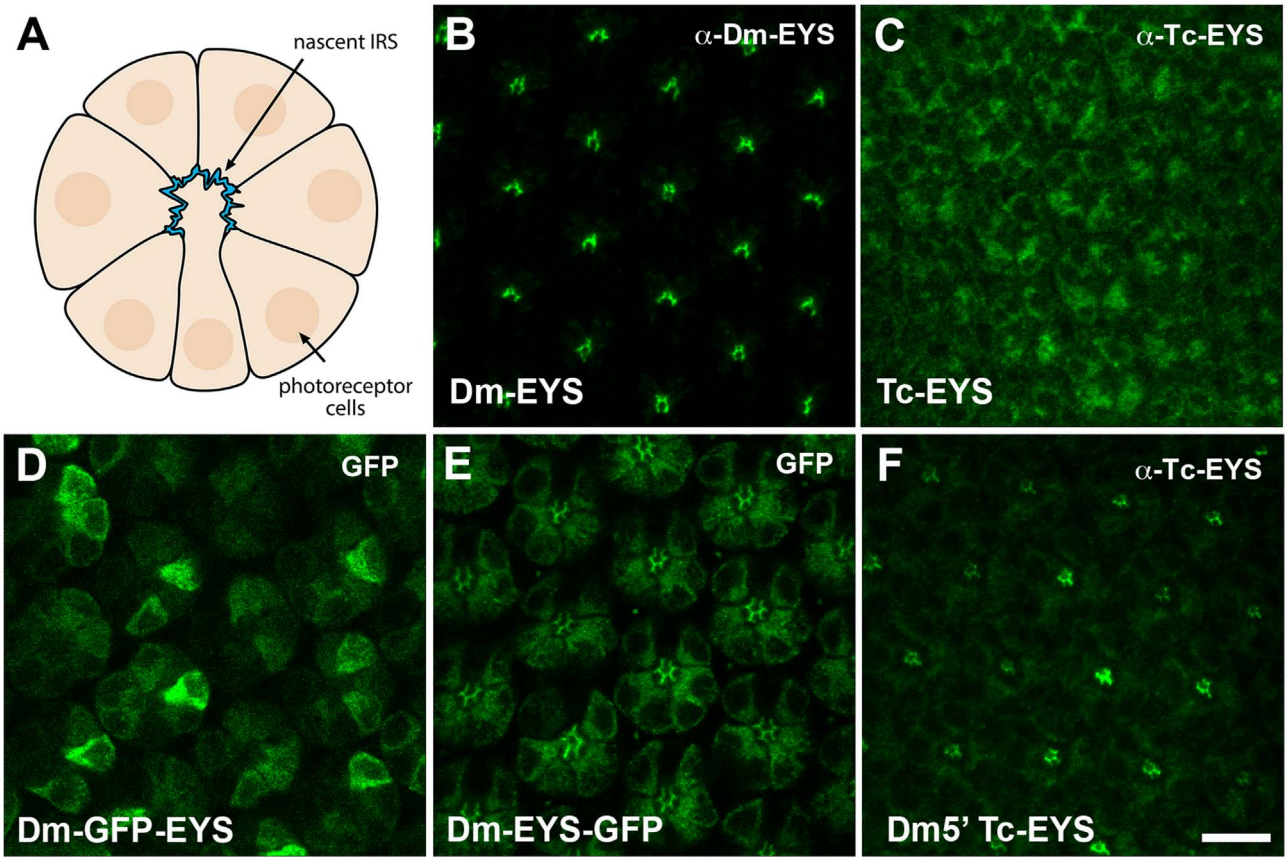

Fig. 4. Immunofluorescence of EYS protein localization in 48 h after puparium formation in wild type photoreceptors. A) Schematic of wild type, B) Dm-EYS, C) Tc-EYS, D) Dm-GFP-EYS, E) Dm-EYS-GFP 1, F) Dm5′Tc-EYS. Each panel represents a single confocal optical section. Scale Bar 10 μm. Genotypes: B) *w* C) *w*; uas Tc-eys/chp-gal4, D) *w; uas Dm-GFP-eys/chp-gal4,* E) *w; uas Dm-eys-GFP/chp-gal4.* F) *w; uas Dm5′Tc-eys/chp-gal4.*

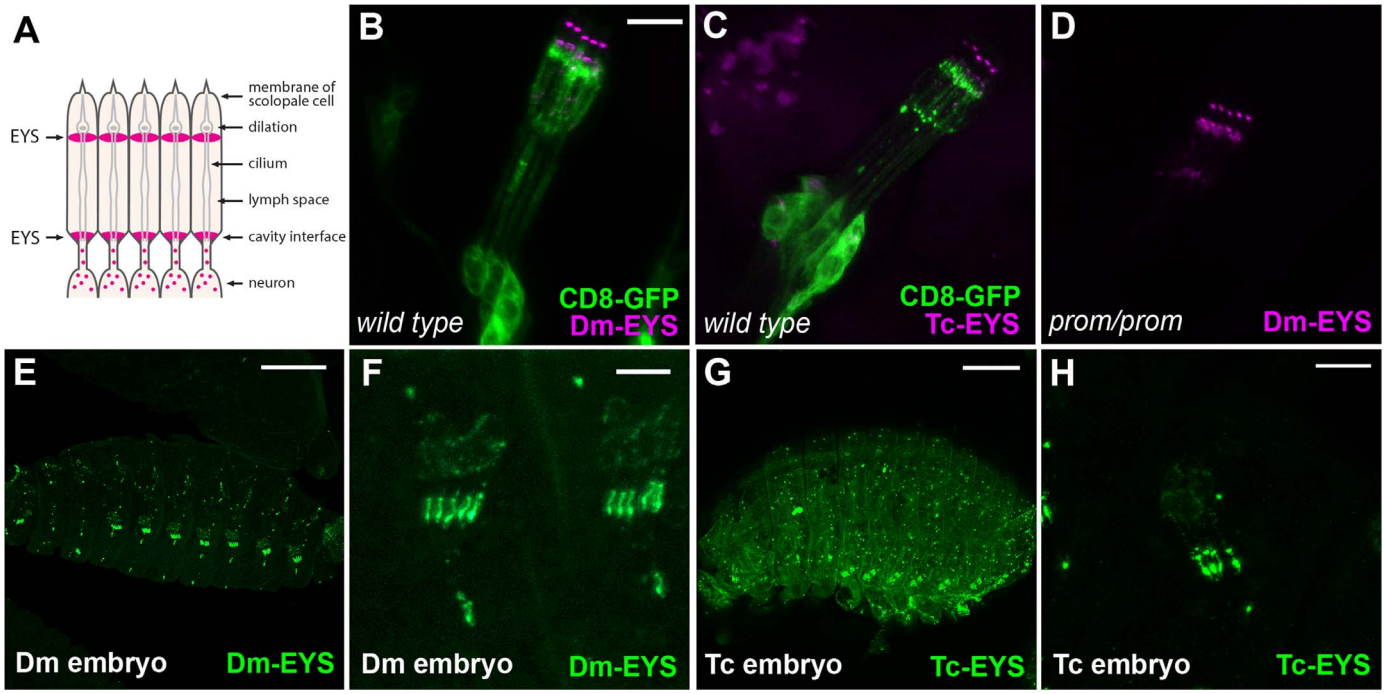

Fig. 5. Localization of EYS in wild type mechanosensory neurons of lateral chordotonal organs. A) Schematic of chordotonal structure, B) ELAV-GAL4, UAS-CD8-GFP (green) and Dm-EYS (magenta) in larval chordotonal organs, C) ELAV-GAL4, UAS-CD8-GFP (green) and Tc-EYS (magenta) in larval chordotonal organs, D) *prominin* mutant and Dm-EYS (magenta) in larval chordotonal organs, E) *Drosophila* embryo and Dm-EYS (Green) Scale Bar 75 μm, F) *Drosophila* embryo and Dm-EYS (Green), Scale Bar 10 μm, G) *Tribolium* embryo and Tc-EYS (Green), Scale Bar 100 μm, H) *Tribolium* embryo and Tc-EYS (Green) Scale Bar 10 μm. Each panel represents a single confocal optical section.

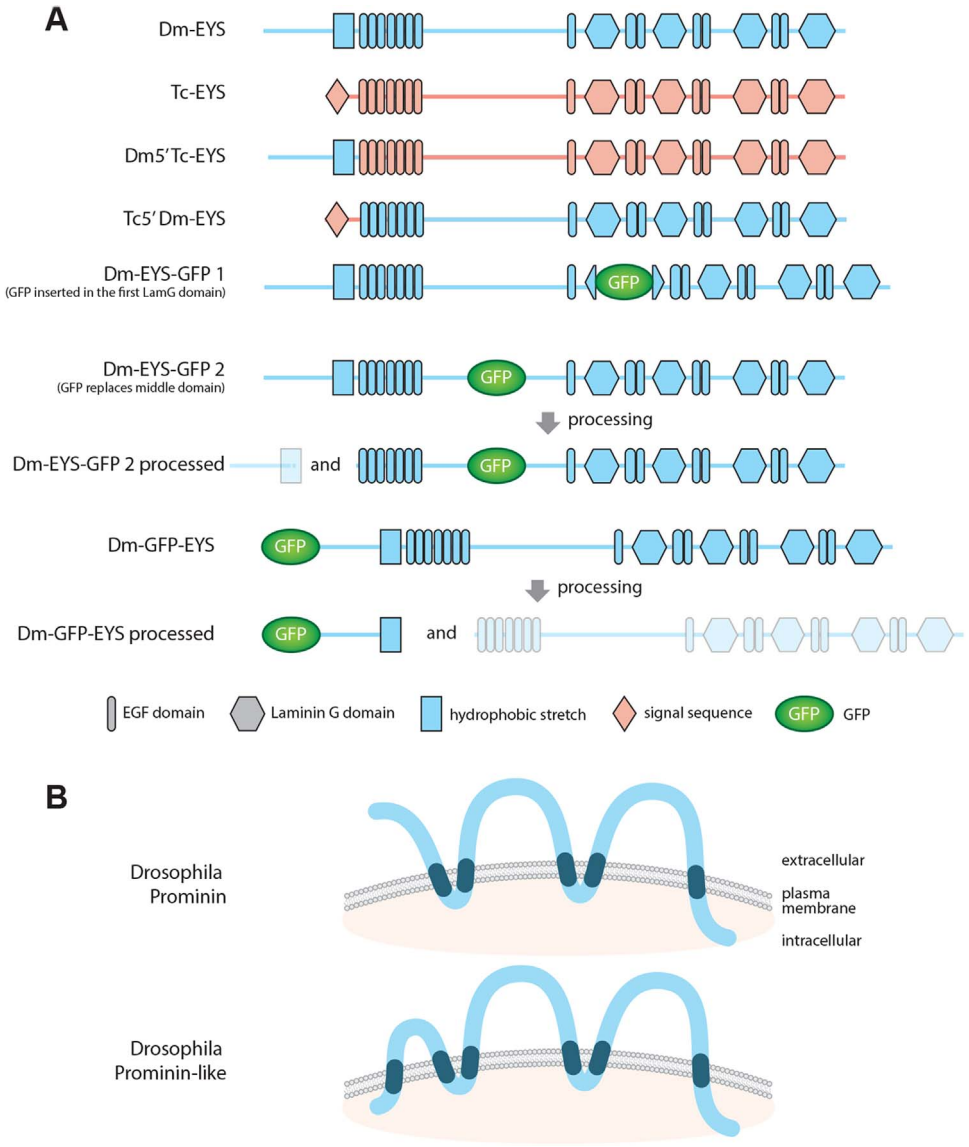

Fig. 6. Schematic and domain organization of EYS and Prominin proteins.

terminus of *Tribolium* EYS, some of the chimeric protein accumulated in the IRS but there was still a failure of complete separation of the rhabdomeres (Fig. 2F). Moreover, immunofluorescence examination demonstrated that this chimera protein, unlike wild type EYS, accumulated abnormally and unevenly throughout the length of the photoreceptor cells (Fig. 8). We conclude that the N-terminus extension of Dm-EYS is a key feature involved in trafficking EYS to the apical membrane.

3.5. Drosophila EYS amino terminus is cleaved upon extracellular release

Secreted EYS is a major component of the IRS. Signal sequences are common in such secreted proteins and are commonly sites for cleavage (Hegde and Bernstein, 2006). We hypothesized that the internalized signal sequence present in Dm-EYS is a site for cleavage, and that the N-terminus extension is removed before subsequent release into the IRS. We first compared the *in vivo* localization of two forms of EYS in which GFP was inserted either before the cleavage site (GFP-EYS), the putative cytoplasmic region of the protein, or after (EYS-GFP) (Nagarkar-Jaiswal et al., 2015), the putative extracellular region of the protein (Fig. 6). When GFP was located in the extracellular region (EYS-GFP) GFP could be detected in the IRS (Fig. 4E) and to a lesser extent on the photoreceptor basal lateral membranes. In contrast, when utilizing the cytoplasmic GFP version (GFP-EYS) GFP was only detected in the photoreceptor cell body and to a lesser extent on the photoreceptor basal lateral membranes. GFP was absent from the IRS (Fig. 4D). Nonetheless, the cytoplasmic GFP tag of the protein, GFP-EYS, retained the capacity to rescue *eys* mutants (Fig. 2G), indicating that the localization pattern was not an artifact of the chimera protein. These data demonstrate that the N-terminus of Dm-EYS is cleaved and remains cytoplasmic, while the remainder of the protein is released extracellularly to form the IRS.

To further assess the dynamics of cleavage and secretion of EYS, we leveraged the previous observation that EYS is only detected extracellularly on *Drosophila* tissue culture cells in the presence of Prominin (Zelhof et al., 2006). Neither Prominin nor EYS is normally expressed in *Drosophila* S2 cells (Cherbas et al., 2011; Graveley et al., 2011). Using our GFP tagged EYS proteins (GFP-EYS and EYS-GFP), we first tested their respective capacities to be secreted and accumulate on S2 cells when co-transfected with Dm-Prominin. In both cases, we observed the accumulation of EYS, as detected by EYS immunofluorescence, on the extracellular region of the cell (Fig. 9B, E). The known epitope/antigen for the EYS antibody, mAb21A6, has been mapped to

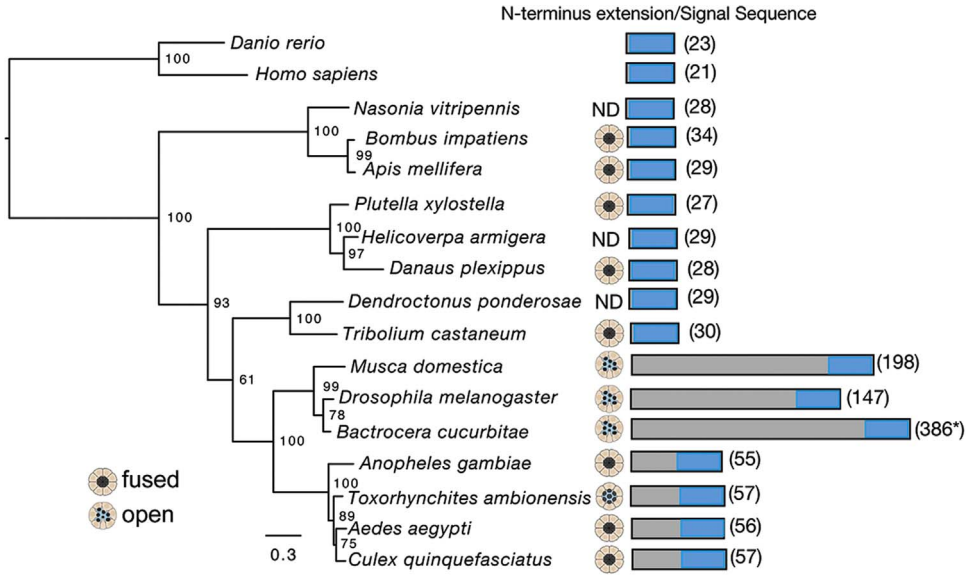

Fig. 7. Comparison of EYS amino terminus extensions among insects. The amino terminus is defined as the leading stretch of amino acids prior to the first cysteine contained within the first EGF domain of the EYS homologs. These regions are mapped onto the phylogeny of insect EYS. Blue boxes represent relative position of predicted signal sequence or internal cleavage sites. Gray boxes represent the amino-terminal extensions present in each species. ND – not determined. * – The extension for *Bactrocera cucurbitae* was not experimentally confirmed as compared for *Musca* and *Drosophila*.

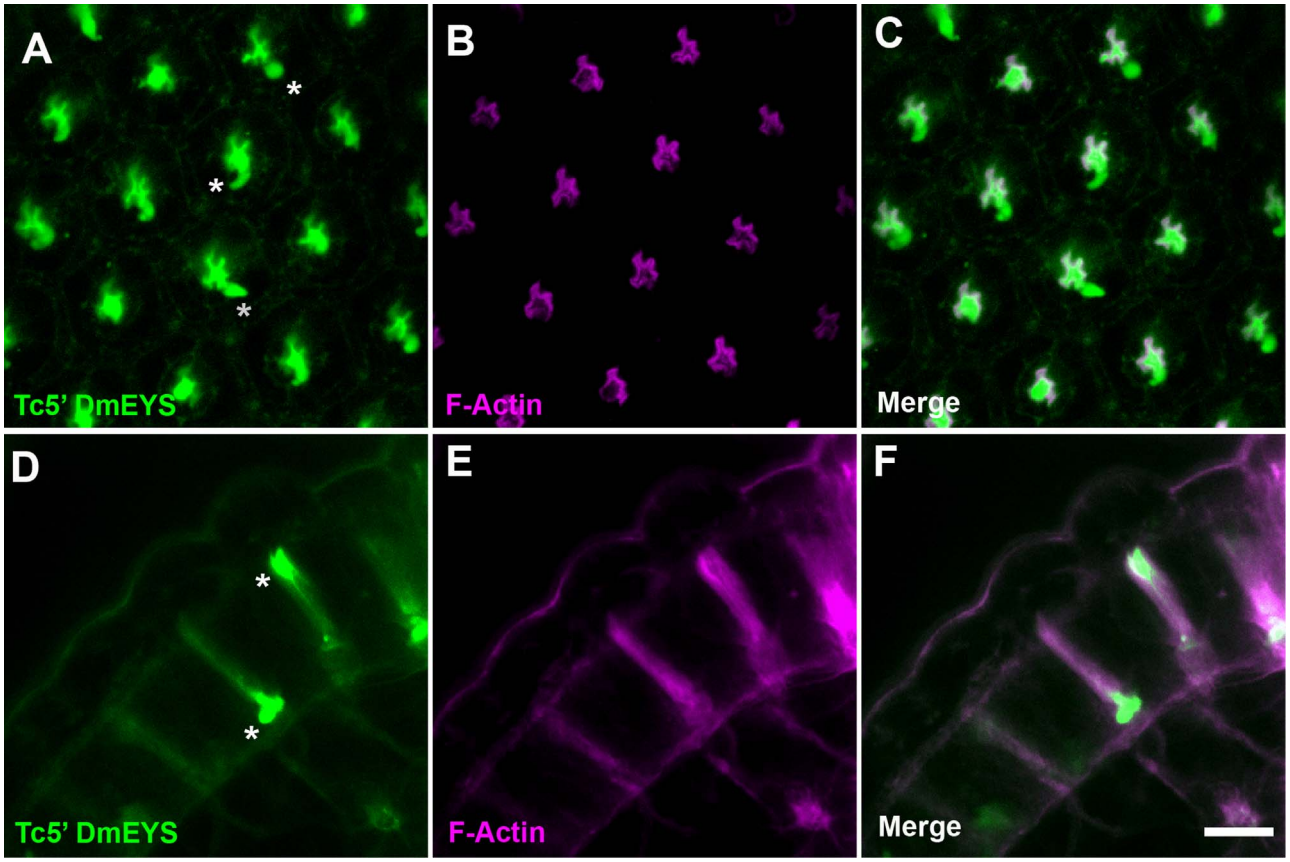

Fig. 8. Mis-localization of Tc5′-DmEYS in developing photoreceptors. Immunofluorescence of Tc5′ DmEYS protein and localization in 52 h after puparium formation (APF) in wild type photoreceptors. A–C) Apical section of developing photoreceptors stained for Tc5′-DmEYS (antibody against Dm-EYS) and Phalloidin to mark F-actin. D–F) Lateral view of developing photoreceptors stained for Tc5′-DmEYS (antibody against Dm-EYS) and Phalloidin. Asterisks mark abnormal accumulation of EYS protein. Each panel represents a single confocal optical section. Scale Bar 10 μm. Genotype: *w; uas Tc5′Dm-eys/chp-gal4*.

the putative extracellular region of EYS between the fifth and seventh EGF repeats of the amino terminus (Zelhof et al., 2006). However, there was a clear difference with respect to the localization of GFP. Only when the GFP tag was located in the putative extracellular region (EYS-GFP) did we observe accumulation of GFP extracellularly and subsequent colocalization with EYS immunofluorescence (Fig. 9A–C). There was no indication that the putative intracellular GFP tag of GFP-EYS was secreted or released extracellularly (Fig. 9D–F). Furthermore,

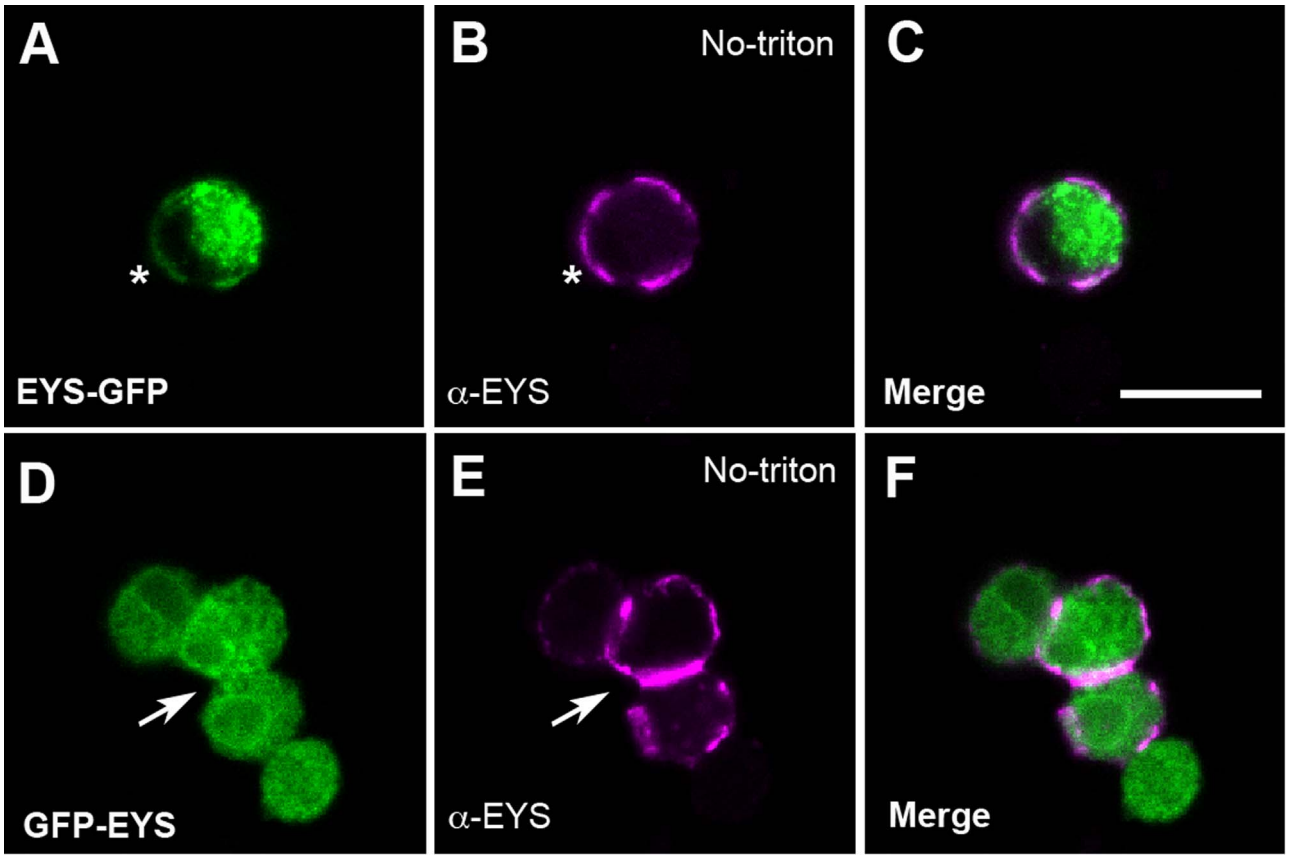

Fig. 9. Examination of GFP epitope tagged versions of Dm-EYS in non-permeabilized tissue culture cells. *Drosophila* S2 cells co-transfected with either (A–C) EYS-GFP, or (D–F) GFP-EYS with Dm-Prominin. GFP localization (A, D) was compared to EYS detection with an antibody (B, E) in the absence of detergent, no cell permeabilization. Asterisk indicates colocalization of GFP and EYS epitope. (C, F) Represent the merged images. Arrow indicates the accumulation of EYS in the absence of corresponding accumulation of GFP. Scale Bar 10 μm.

when we examined the intracellular pool of each tagged protein, we observed two distinct signals for GFP and EYS with the GFP-EYS construct, indicating that GFP is removed from the GFP-EYS chimera protein. Conversely, we observed only a single colocalization signal with EYS-GFP (Fig. 10). The cleavage was also verified by Western analysis. In cell extracts expressing GFP-EYS we detected a proteolytic cleavage product associated with GFP-EYS of the expected size of GFP plus the additional 147 amino acids prior to and adjacent to the hydrophobic stretch (Figs. 11 and 6). Together, our results demonstrate that the internalized signal sequence in Dm-EYS is a cleavage site which is processed before EYS is secreted. In addition, Prominin is required for the retention of secreted EYS on the extracellular surface, but the processing of EYS occurred in the absence of Prominin in cell culture (Fig. 11). This finding is consistent with our observation that the loss of Prominin had no effect on the localization of Dm-EYS in mechanosensory organs (Fig. 5D) or the ability of Dm-EYS to be targeted to and secreted in the absence of Prominin (Zelhof et al., 2006).

3.6. IRS formation is dependent upon specific interactions between EYS and a subset of Prominin paralogs

The failure of Tc-EYS to rescue the *eys* photoreceptor mutant even when properly directed to the apical membrane suggested that additional mechanisms are required for the transition from a fused to an open rhabdom. Previous data have demonstrated that the interaction between EYS and Prominin is critical for IRS formation (Nie et al., 2012; Zelhof et al., 2006). In particular, Prominin was proposed to be a "receptor" for EYS ensuring proper distribution of EYS during the transformation of the photoreceptor apical membrane into a rhabdomere. Therefore, the lack of rescue observed with Tc-EYS or Dm5′Tc-EYS could be due to a failure of Tc-EYS to interact with *Drosophila* Prominin as observed with the human homologs (Nie et al., 2012). To examine this possibility, we tested whether either Tc-EYS or Dm5′Tc-EYS could be detected extracellularly on S2 cells in the presence of Dm-Prominin. In both cases, even though protein expression can be detected in S2 cells, neither protein was detected on the surface of the cell, suggesting that the interaction between EYS and Prominin required for the proper secretion and positioning of EYS may be highly specific (Fig. 12).

Given the specific interaction between Dm-EYS and Dm-Prominin, we further tested whether open rhabdoms may also correlate with structural changes in Prominin. We performed genome searches and phylogenetic analyses of Prominin homologs from selected holometabolous insects. Our analysis revealed two distinct clades of Prominin homologs across holometabolous insects, Prominin and Prominin-like, as known from *Drosophila* (Fig. 13). Prominin-like loci were lost in a few lineages, but Prominin is present in each species, with duplications noted in lepidopteran species. Thus, the presence of Prominin or Prominin-like did not correlate with the presence of open or fused rhabdoms. Structurally, the analyses of Prominin and Prominin-like proteins demonstrate well supported, highly divergent transmembrane domain structures. Whereas Prominin clade proteins contain five transmembrane domains, Prominin-like has a predicted sixth transmembrane domain (Fig. 6).

We hypothesized that Prominin and Prominin-like were not functionally equivalent based on structural differences observed between the different gene families. Utilizing similar expression conditions, Dm-Prominin-like was not capable of rescuing *prominin* mutants (Fig. 14A–C), even though Dm-Prominin-like localized to the

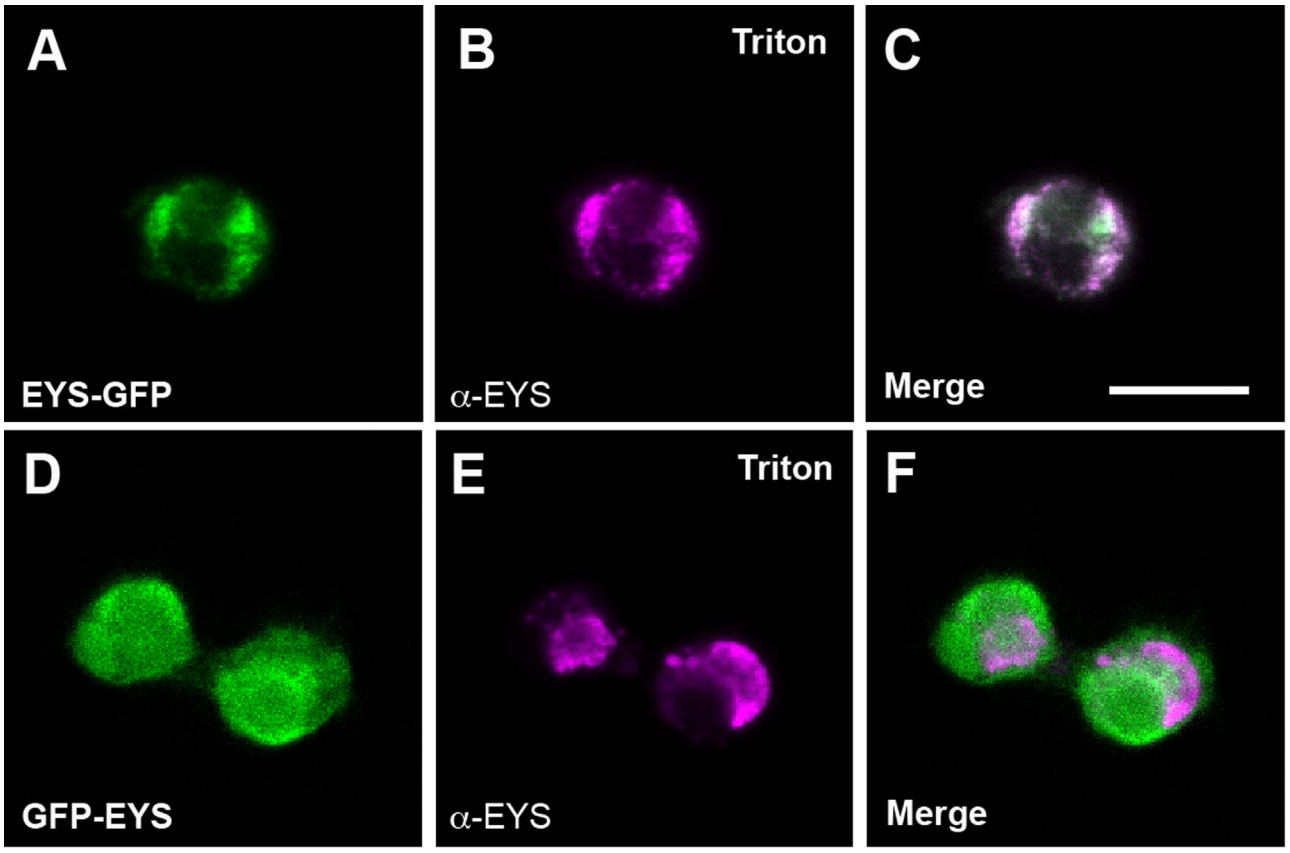

Fig. 10. Examination GFP epitope tagged versions of Dm-EYS in permeabilized *Drosophila* tissue culture cells. *Drosophila* S2 cells transfected with either (A–C) EYS-GFP, or (D–F) GFP-EYS. GFP localization (A, D) was compared to EYS detection with an antibody (B, E) in the presence of detergent, cell permeabilization. (C, F) Represent the merged images. Scale Bar 10 μm.

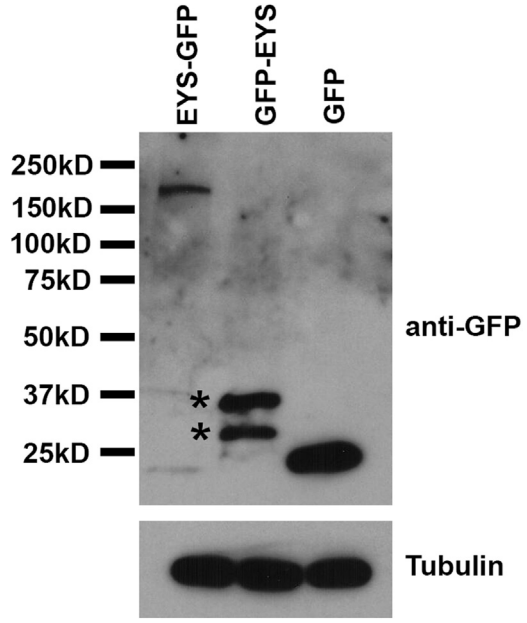

Fig. 11. Dm-EYS proteolytic cleavage products are detected in *Drosophila* tissue culture cells. Immunoprecipitation and detection of GFP from *Drosophila* S2 cells transfected with either EYS-GFP, GFP-EYS, or GFP in the absence of Dm-Prominin. Asterisks indicate intracellular GFP containing cleavage products associated only with GFP-EYS.

apical photoreceptor membrane during rhabdomere morphogenesis (Fig. 15). Together, these results reveal significant structural diversity and a lack of functional equivalency among Prominin paralogs. Interestingly, this pattern of structural variation among holometabolous insect Prominin homologs suggests the potential for novel, species-specific interactions between EYS and Prominin in the adaptive evolution of rhabdom architectures.

4. Discussion

4.1. In holometabolous insects, open rhabdoms are evolutionary innovations based on the co-option of EYS from an ancestral role in mechanosensory neurons

Our phylogenetic comparative analyses strongly support the hypothesis that the open rhabdom configuration is a derived condition in holometabolous insects (Fig. 1). We also show that the role of EYS in mechanosensory neurons is conserved between *Drosophila* and *Tribolium* and was co-opted in *Drosophila* photoreceptor cells for the generation of the IRS. We found that EYS expression and subcellular localization is conserved in mechanosensory neurons of both *Tribolium* and *Drosophila*, particularly in the lateral chordotonal organs of developing embryos. Interestingly, despite sequence differences, proteins from either species were capable of functioning in *Drosophila* mechanosensory neurons, but only the *Drosophila* protein (Dm-EYS) was fully functional in *Drosophila* photoreceptors.

EYS is an evolutionary conserved gene found outside of insects. EYS homologs are characterized by an amino terminus containing EGF repeats, a divergent central domain, and a carboxy terminus of alternating EGF and Laminin G domains. However, in brachycheran dipterans, EYS has an additional amino terminus extension that leads to the internalization of the signal sequence. Like *Tribolium*, both human and Zebrafish EYS have typical, exposed, signal sequences of 21 and 23 amino acids, respectively, which function in secretion (Abd El-

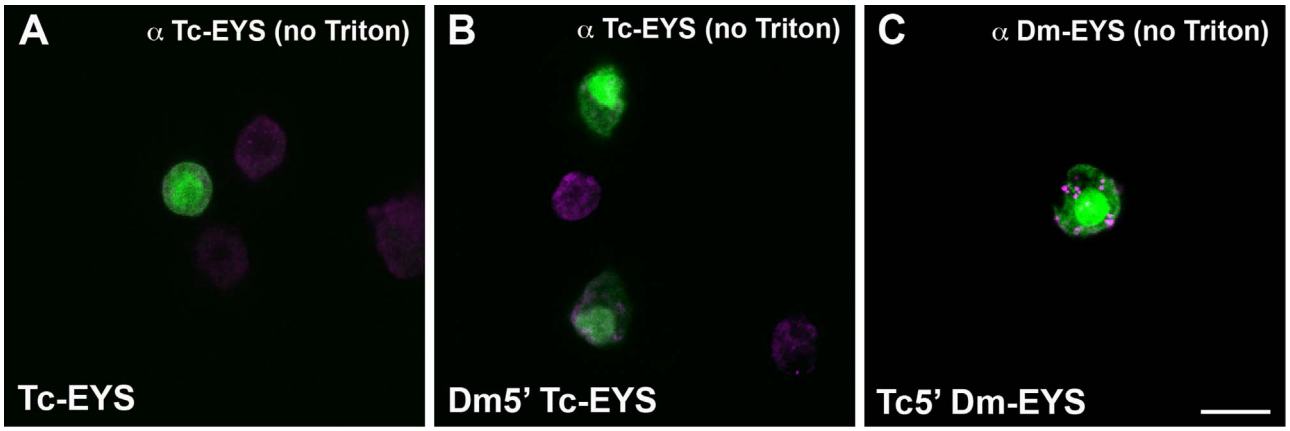

Fig. 12. Tc-EYS and Dm5′-Tc-EYS do not accumulate extracellularly in the presence of Dm-Prominin in Drosophila tissue culture cells. *Drosophila* S2 cells transfected with either (A) Tc-EYS, (B) Dm5'-Tc-EYS, and (C) Tc5'-Dm-EYS in the presence of Dm-Prominin and cytoplasmic GFP. In the absence of detergent (Triton) only Tc5′ Dm-EYS is detected extracellularly on the transfected cells. There is no difference between background fluorescence between transfected and non-transfected cells containing Tc-EYS or Dm5'-Tc-EYS. Scale Bar 10 μm.

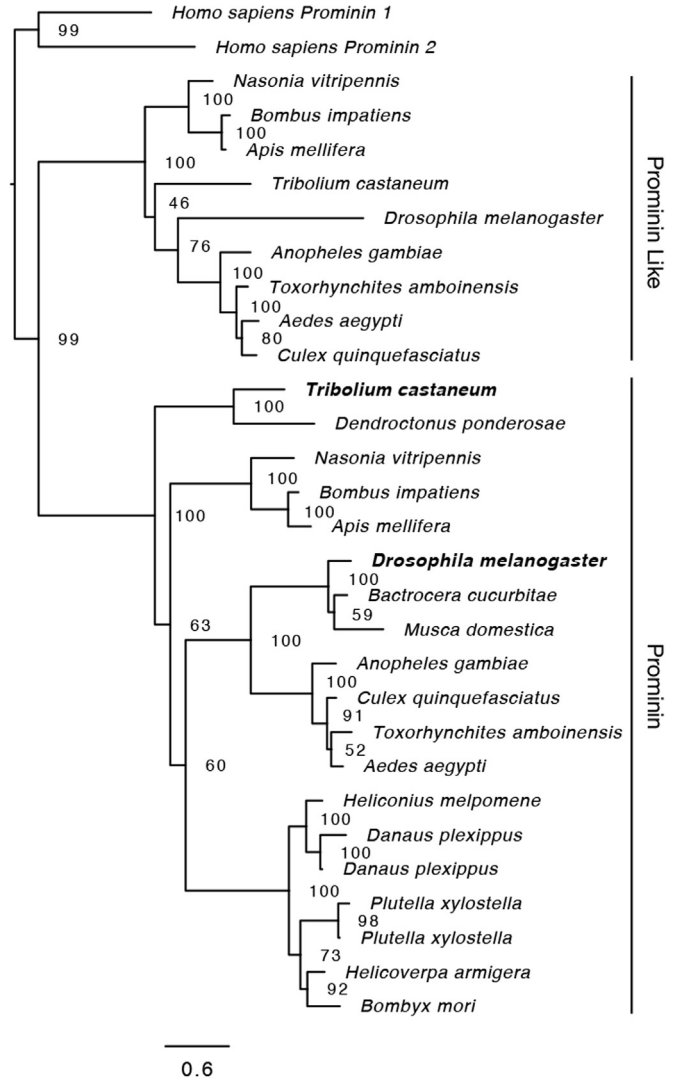

Fig. 13. Phylogenetic analyses of Prominin and Prominin-like proteins. Both clades are present across holometabolous insects, irrespective of rhabdom morphology. Prominin is present in all taxa examined but Prominin-like has been lost in *Bactrocera cucurbitae*, *Musca domestica* and all lepidopterans. Prominin gene duplicates are also retained in some lepidopterans.

Aziz et al., 2008; Collin et al., 2008; Lu et al., 2017; Yu et al., 2016). Another feature of most EYS homologs studied to date is that they are expressed by ciliated neurons. In deuterostomes, EYS expression is limited to ciliary photoreceptors where it is involved in maintaining the integrity of the ciliary projections (Abd El-Aziz et al., 2008; Collin et al., 2008; Lu et al., 2017; Yu et al., 2016). In insects, mechanosensitive neurons are also ciliated and EYS functions to preserve chordotonal neuron cell shape in the face of temperature, osmotic or chemical stress (Cook et al., 2008). In both systems, EYS is involved in protecting the integrity of ciliary projections among different types of sensory neurons. Our results suggest that in brachycerans, EYS took on a new role as a major component of the IRS through co-option for function in rhabdomeric photoreceptors.

4.2. Internalization of signal sequence for cleavage: a novel mechanism for the evolution of adaptive rhabdom configurations

Our results demonstrate that the evolution of a novel N-terminus extension of EYS that effectively buries the secretion signal sequence was essential for the transition to an open rhabdom configuration in brachycerans. Signal sequences for export are typically 15–30 amino acids in length and have low sequence homology, but contain three characteristic domains: a basic, hydrophobic, and polar domain. In addition to signaling a given protein for secretion, signal sequences can provide other forms of information, including trafficking (Hegde and Bernstein, 2006; Voss et al., 2013). In *Drosophila*, we demonstrated that an alteration in the localization of the EYS signal sequence is critical for the transition from fused to open rhabdoms. Across holometabolous insects EYS has a typical 15–30 amino acid signal sequence at the N-terminus of the protein. In *Drosophila* and other brachyceran EYS proteins this signal sequence is internalized by a novel N-terminus extension that is greater than 100 amino acids in length in some species. Our data show that this N-terminus extension is responsible for proper targeting of EYS to the apical membrane and is cleaved prior to secretion. This N-terminus extension has no effect on function in mechanosensory neurons but is necessary for proper targeting of EYS to the apical membrane in *Drosophila* photoreceptors. When Tc-EYS is expressed in *eys* mutant photoreceptor cells, only a slight separation of the rhabdomeric stalk membranes closest to the adherens junctions (Fig. 2D) is observed. Therefore, the signal sequence alone was able to direct a limited portion of Tc-EYS to be secreted, while the majority of Tc-EYS remained intracellularly localized to regions other than the apical membrane at the critical period of IRS formation (Fig. 4C). The replacement of the N-terminus of Dm-EYS with Tc-EYS resulted in the chimeric protein being targeted to the

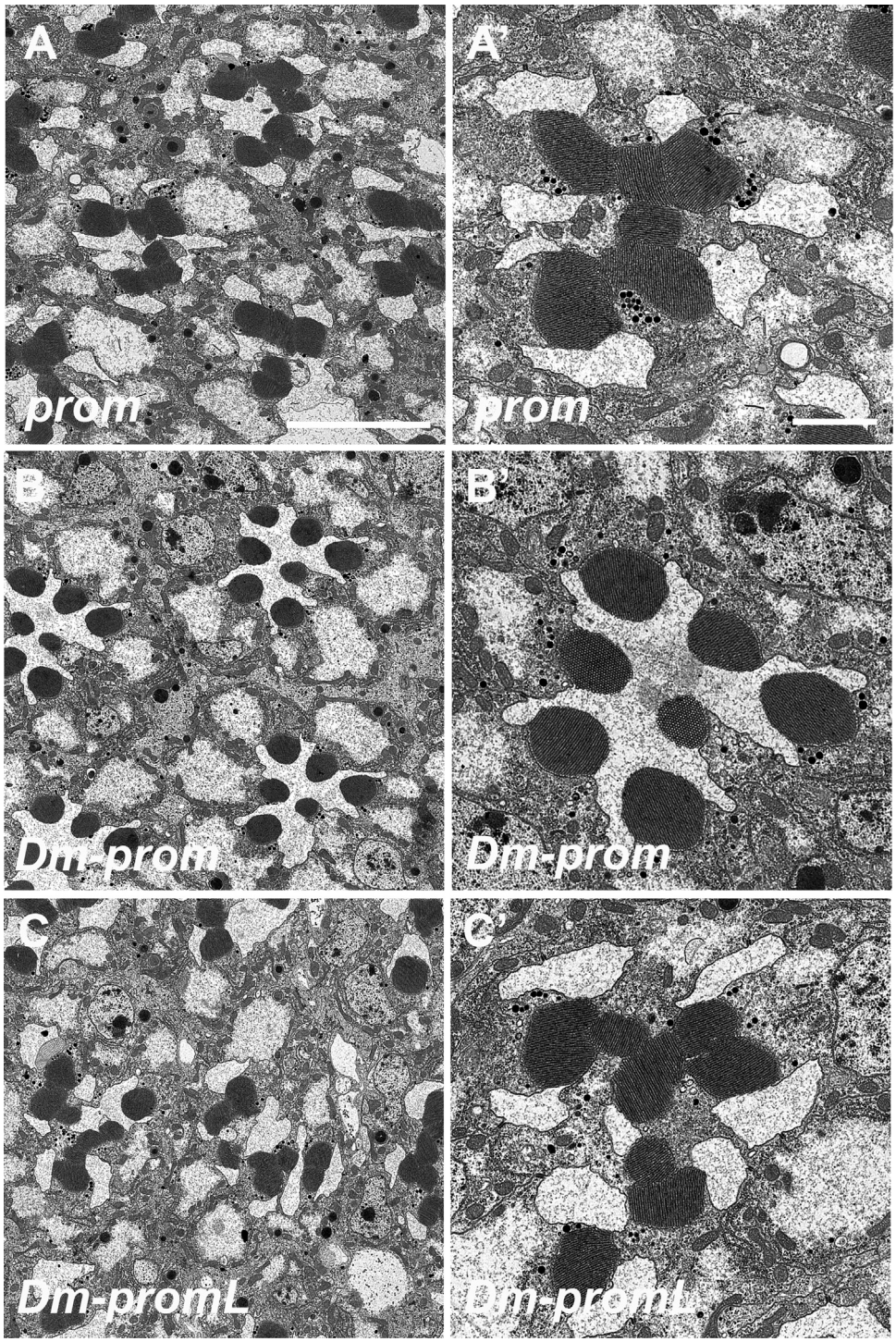

Fig. 14. Prominin and Prominin-like are not functionally equivalent. Transmission electron micrographs of adult *Drosophila* ommatidia. A) *prom* mutant, B) Rescue with Dm-prominin, C) Rescue with Dm-prominin-like. A′–C′ represent higher magnifications of each panel. Scale Bars 5 μm and 2 μm. Genotypes: A) *w; prom^1/prom^1*, B) *w; prom^1/prom^1; prom-gal4/* uas-Dm-*prominin*, C) *w; prom^1/prom^1; prom-gal4/* uas-Dm-*prominin-like.*

photoreceptor apical surface. However, despite correct targeting, Dm5-Tc-EYS was not capable of rescuing *eys* mutants, suggesting other factors are required. Conversely, the replacement of the Dm-EYS N-terminus with the Tc-EYS signal sequence also resulted in an incomplete separation, but in these experiments the failure to rescue *eys* mutants was due to mis-targeting of EYS to other regions of the developing photoreceptors (Fig. 8). Therefore, a typical signal sequence is not sufficient to target EYS to the apical photoreceptor membrane, suggesting a novel, presently unknown trafficking mechanism.

Moreover, this putative trafficking mechanism may not be limited to targeting EYS in open rhabdom systems. In addition to the IRS, one important feature of open rhabdoms is that the apical photoreceptor membrane is divided into two distinct domains, the rhabdomere and the stalk membrane, the latter of which is devoid of microvilli. The generation of the stalk membrane is dependent on the transmembrane protein Crumbs (Izaddoost et al., 2002; Johnson et al., 2002; Pellikka et al., 2002), which localizes to the entire stalk membrane. Like *Drosophila* EYS, *Drosophila* Crumbs has an internalized cleavable signal sequence with an 83 N-terminus extension. This extension, like EYS, is not present in Crumbs homologs from species with fused

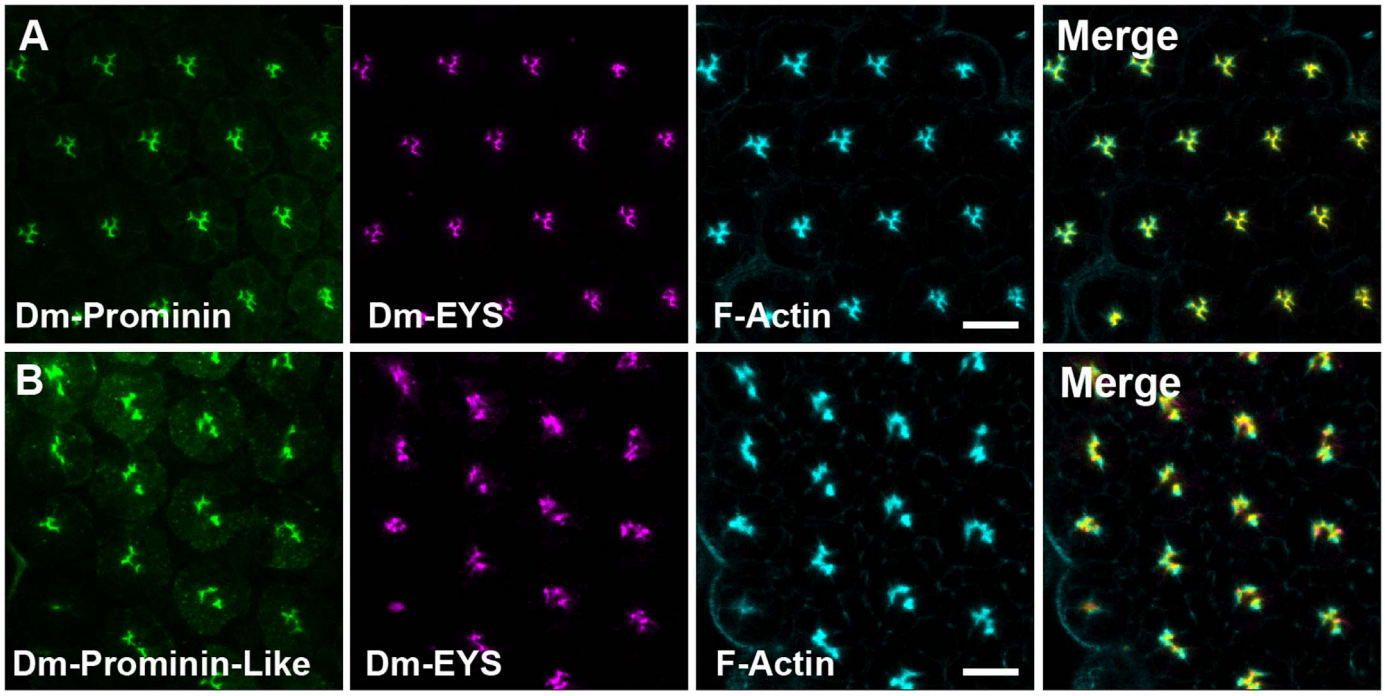

Fig. 15. Localization of Prominin and Prominin-like in *Drosophila* photoreceptors. A) Immunofluorescence of Dm-Prominin (green) in wild type photoreceptors at 48 h after puparium formation countered stained with Dm-EYS (magenta) and F-Actin (blue). B) Immunofluorescence of Dm-Prominin-like (green) in *prominin* mutant photoreceptors at 48 h after puparium formation countered stained with Dm-EYS (magenta) and F-Actin (blue). Scale Bar 10 μm. Genotypes: A) *w*, B) *w; prom^{1}/prom^{1}; prom-gal4/* uas-Dm-*prominin-like*.

rhabdoms. Crumbs proteins from speices with fused rhabdoms including *Tribolium castaneum*, *Aedes aegypti* and *Nasonia vitripennis* all have typical signal sequences of 22, 25, and 22, amino acids, respectively, as is also present human Crumbs proteins (Kilic et al., 2010). To date the sufficiency and necessity of this N-terminus extension in Crumbs has not been tested in *Drosophila* photoreceptors.

4.3. Prominin orthologs are not interchangeable

It is intriguing that the chimeric protein Dm5-Tc-EYS (Tc-EYS with the N-terminus extension of Dm-EYS) localized correctly to the apical membrane in *Drosophila* photoreceptors but was still unable to rescue the *eys* mutant as it failed to generate an inter-rhabdomeral space. Conversely, the chimera Tc5-Dm-EYS, which lacks the targeting signal altogether but has an otherwise wild type EYS, was capable of generating a partial IRS. Why is correct targeting to the apical membrane not sufficient to rescue *eys* mutants? Prominin has been hypothesized to be a receptor for EYS, but detailed studies of how Prominin promotes the secretion and/or accumulation of EYS have not been done. We hypothesize that, together with the change in tissue expression and protein structure in Dm-EYS, an additional specific protein-protein interaction between EYS and Prominin must have evolved to facilitate the proper deployment of EYS and the development of the IRS in the open rhabdom systems of brachycerans, including *Drosophila*. Our results from cell culture and *in vivo* studies show that the Prominin orthologs examined are not functionally equivalent and we confirmed the species-specific nature of EYS-Prominin interactions in cell culture experiments where Tc-EYS and Dm-Prominin did not interact in a manner that resulted in the proper deployment of EYS, but Dm-EYS and Dm-Prominin were able to do so. Our results are also an agreement with previous experiments that tested the functional equivalency of the human homologs EYS and Prominin-1 (Nie et al., 2012) in *Drosophila* photoreceptors. Whereas, human Prominin-1 was functionally equivalent to Dm-Prominin, human EYS alone did not rescue *eys* mutants.

4.4. Mechanism and conservation across all open rhabdoms

Our data clarify several features of the evolutionary and developmental origins of the open rhabdoms of brachycerans while, at the same time, introducing numerous unanswered questions. We demonstrate a critical role for the N-terminus extension in the correct targeting of EYS to the photoreceptor apical domain in *Drosophila*. However, while this N-terminus extension is present in the predicted EYS sequences of several drosophilid speices with sequenced genomes this extension has only been experimentally confirmed in two brachyceran species, *Musca domestica* and *Drosophila melanogaster*. The N-terminus extensions of these species are highly divergent and do not indicate shared sequence motifs, raising questions about a putative, shared cellular mechanism for targeting. Future studies will experimentally confirm the N-terminus sequence from a diversity of brachyceran EYS sequences and utilize *Drosophila* to genetically dissect the sequence features critical for targeting and secretion to the IRS. In addition, the importance of the N-terminal extension in the development of open rhabdoms in non-brachyceran dipterans is also questionable. Each of the EYS sequences sampled from mosquitoes (Nematocera) have similar N-terminal extensions, albeit shorter as compared to *Drosophila*, but only *Toxorhynchites* has an open rhabdom (Land et al., 1999). It is likely that other mechanisms, possibly involving interactions between EYS and Prominin, underlie the open rhabdome configuration of *Toxorhynchites*.

5. Conclusions

Understanding how adaptive morphologies originate is a central question in evolutionary developmental biology. Once focused largely on the relative roles of protein coding *vs*. regulatory mutations as drivers of novel trait evolution (Carroll, 2008; Hoekstra and Coyne, 2007; Stern and Orgogozo, 2008), a more complex mutational landscape involving both factors is likely involved for many traits. Our study exemplifies this as we outline a mosaic of concomitant mutations that underlie the evolution of an open rhabdom from a fused rhabdom

configuration in brachyceran dipterans. These alterations, each necessary, profoundly affect the cell biology of developing photoreceptor cells resulting in the secretion of EYS and the expansion of the IRS. First, regulatory innovations must have led to the expansion of EYS expression from mechanosensory organs, as in *Tribolium*, *Drosophila* and presumably other insects, to include photoreceptor expression, in *Drosophila* and other brachycerans. Second, in order for EYS to be targeted to the apical membrane of photoreceptor cells, the evolution of an N-terminus extension was required. This N-terminus extension, present in brachyceran taxa with open rhabdoms, does not directly contribute to the IRS, but is necessary for proper targeting of EYS to the apical membrane. Finally, specific protein-protein interactions evolved between EYS and Prominin that facilitate the proper deployment of secreted, cleaved, EYS to the IRS. Our data indicate an evolutionary transition involving both non-coding and coding changes that resulted in a novel visual architecture and permitted a subset of diurnal dipteran lineages to diversify into niches that require high acuity vision.

Acknowledgments

We thank Dr. Jason Pitts for *Toxorhynchites amboinensis* material and sequence data and the Bloomington Drosophila Stock Center and the Drosophila Genomics Resource Center for reagents. We thank Dr. J. Powers and the Indiana University Light Microscopy Center for assistance with image generation. This work was supported by National Science Foundation IOS-1353267 (ACZ) and National Science Foundation DOB-1638296 (DCP).

References

Abd El-Aziz, M.M., Barragan, I., O'Driscoll, C.A., Goodstadt, L., Prigmore, E., Borrego, S., Mena, M., Pieras, J.I., El-Ashry, M.F., Safieh, L.A., Shah, A., Cheetham, M.E., Carter, N.P., Chakarova, C., Ponting, C.P., Bhattacharya, S.S., Antinolo, G., 2008. EYS, encoding an ortholog of Drosophila spacemaker, is mutated in autosomal recessive retinitis pigmentosa. Nat. Genet. 40, 1285–1287.

Agi, E., Langen, M., Altschuler, S.J., Wu, L.F., Zimmermann, T., Hiesinger, P.R., 2014. The evolution and development of neural superposition. J. Neurogenet. 28, 216–232.

Altschul, S.F., Gish, W., Miller, W., Myers, E.W., Lipman, D.J., 1990. Basic local alignment search tool. J. Mol. Biol. 215, 403–410.

Braitenberg, V., 1967. Patterns of projection in the visual system of the fly. I. Retina-lamina projections. Exp. Brain Res. 3, 271–298.

Brammer, J.D., 1970. The ultrastructure of the compound eye of a mosquito Aedes aegypti L.. J. Exp. Zool. 175, 181–195.

Brown, S.J., Shippy, T.D., Miller, S., Bolognesi, R., Beeman, R.W., Lorenzen, M.D., Bucher, G., Wimmer, E.A., Klingler, M., 2009. The red Flour beetle, Tribolium castaneum (Coleoptera): a model for studies of development and pest biology. Cold Spring Harb. Protoc., (pdb.emo126-).

Carroll, S.B., 2008. Evo-devo and an expanding evolutionary synthesis: a genetic theory of morphological evolution. Cell 134, 25–36.

Cherbas, L., Willingham, A., Zhang, D., Yang, L., Zou, Y., Eads, B.D., Carlson, J.W., Landolin, J.M., Kapranov, P., Dumais, J., Samsonova, A., Choi, J.H., Roberts, J., Davis, C.A., Tang, H., van Baren, M.J., Ghosh, S., Dobin, A., Bell, K., Lin, W., Langton, L., Duff, M.O., Tenney, A.E., Zaleski, C., Brent, M.R., Hoskins, R.A., Kaufman, T.C., Andrews, J., Graveley, B.R., Perrimon, N., Celniker, S.E., Gingeras, T.R., Cherbas, P., 2011. The transcriptional diversity of 25 Drosophila cell lines. Genome Res. 21, 301–314.

Collin, R.W., Littink, K.W., Klevering, B.J., van den Born, L.I., Koenekoop, R.K., Zonneveld, M.N., Blokland, E.A., Strom, T.M., Hoyng, C.B., den Hollander, A.I., Cremers, F.P., 2008. Identification of a 2 Mb human ortholog of Drosophila eyes shut/spacemaker that is mutated in patients with retinitis pigmentosa. Am. J. Hum. Genet. 83, 594–603.

Cook, B., Hardy, R.W., McConnaughey, W.B., Zuker, C.S., 2008. Preserving cell shape under environmental stress. Nature 452, 361–364.

Eguchi, E., Naka, K.I., Kuwabara, M., 1962. The development of the rhabdom and the appearance of the electrical response in the insect eye. J. Gen. Physiol. 46, 143–157.

Friedrich, M., 2010. Evolution of Visual Performance-associated Genes in Drosophila. Encyclopedia of Life Sciences (ELS).

Gramates, L.S., Marygold, S.J., Santos, G.D., Urbano, J.M., Antonazzo, G., Matthews, B.B., Rey, A.J., Tabone, C.J., Crosby, M.A., Emmert, D.B., Falls, K., Goodman, J.L., Hu, Y., Ponting, L., Schroeder, A.J., Strelets, V.B., Thurmond, J., Zhou, P., the FlyBase, C., 2017. FlyBase at 25: looking to the future. Nucleic Acids Res. 45, D663–D671.

Graveley, B.R., Brooks, A.N., Carlson, J.W., Duff, M.O., Landolin, J.M., Yang, L., Artieri, C.G., van Baren, M.J., Boley, N., Booth, B.W., Brown, J.B., Cherbas, L., Davis, C.A., Dobin, A., Li, R., Lin, W., Malone, J.H., Mattiuzzo, N.R., Miller, D., Sturgill, D., Tuch, B.B., Zaleski, C., Zhang, D., Blanchette, M., Dudoit, S., Eads, B., Green, R.E., Hammonds, A., Jiang, L., Kapranov, P., Langton, L., Perrimon, N., Sandler, J.E., Wan, K.H., Willingham, A., Zhang, Y., Zou, Y., Andrews, J., Bickel, P.J., Brenner, S.E., Brent, M.R., Cherbas, P., Gingeras, T.R., Hoskins, R.A., Kaufman, T.C., Oliver, B., Celniker, S.E., 2011. The developmental transcriptome of Drosophila melanogaster. Nature 471, 473–479.

Gurudev, N., Yuan, M., Knust, E., 2014. Chaoptin, prominin, eyes shut and crumbs form a genetic network controlling the apical compartment of Drosophila photoreceptor cells. Biol. Open 3, 332–341.

Hegde, R.S., Bernstein, H.D., 2006. The surprising complexity of signal sequences. Trends Biochem. Sci. 31, 563–571.

Hoekstra, H.E., Coyne, J.A., 2007. The locus of evolution: evo devo and the genetics of adaptation. Evolution 61, 995–1016.

Husain, N., Pellikka, M., Hong, H., Klimentova, T., Choe, K.M., Clandinin, T.R., Tepass, U., 2006. The agrin/perlecan-related protein eyes shut is essential for epithelial lumen formation in the Drosophila retina. Dev. Cell 11, 483–493.

Izaddoost, S., Nam, S.C., Bhat, M.A., Bellen, H.J., Choi, K.W., 2002. Drosophila crumbs is a positional cue in photoreceptor adherens junctions and rhabdomeres. Nature 416, 178–183.

Johnson, K., Grawe, F., Grzeschik, N., Knust, E., 2002. Drosophila crumbs is required to inhibit light-induced photoreceptor degeneration. Curr. Biol. 12, 1675–1680.

Katoh, K., Standley, D.M., 2016. A simple method to control over-alignment in the MAFFT multiple sequence alignment program. Bioinformatics 32, 1933–1942.

Kilic, A., Klose, S., Dobberstein, B., Knust, E., Kapp, K., 2010. The Drosophila Crumbs signal peptide is unusually long and is a substrate for signal peptide peptidase. Eur. J. Cell Biol. 89, 449–461.

Kirschfeld, K., 1967. The projection of the optical environment on the screen of the rhabdomere in the compound eye of the Musca. Exp. Brain Res. 3, 248–270.

Land, M.F., Gibson, G., Horwood, J., Zeil, J.J.J.o.C.P.A., 1999. Fundamental differences in the optical structure of the eyes of nocturnal and diurnal mosquitoes. J. Comp. Phys. A 185, 91–103.

Land, M.F., Horwood, J., 2005. Different retina-lamina projections in mosquitoes with fused and open rhabdoms. J. Comp. Physiol. A Neuroethol. Sens. Neural Behav. Physiol. 191, 639–647.

Land, M.F., Nilsson, D.E., 2002. Animal Eyes. Oxford University Press.

Liu, H., Deng, S., Zhao, X., Cao, F., Lu, Y., 2017. Structure and photoreception mechanism of the compound eye of Bactrocera dorsalis Hendel. J. South China Agric. Univ. 38, 75–80.

Lu, Z., Hu, X., Liu, F., Soares, D.C., Liu, X., Yu, S., Gao, M., Han, S., Qin, Y., Li, C., Jiang, T., Luo, D., Guo, A.Y., Tang, Z., Liu, M., 2017. Ablation of EYS in zebrafish causes mislocalisation of outer segment proteins, F-actin disruption and cone-rod dystrophy. Sci. Rep. 7, 46098.

McCulloch, K.J., Osorio, D., Briscoe, A.D., 2016. Sexual dimorphism in the compound eye of Heliconius erato: a nymphalid butterfly with at least five spectral classes of photoreceptor. J. Exp. Biol. 219, 2377–2387.

Meyer-Rochow, V.B., 1981. Electrophysiology and histology of the eye of the bumblebee Bombus hortorum (L.) (Hymenoptera: Apidae). J. R. Soc. N.Z. 11, 123–153.

Misof, B., Liu, S., Meusemann, K., Peters, R.S., Donath, A., Mayer, C., Frandsen, P.B., Ware, J., Flouri, T., Beutel, R.G., Niehuis, O., Petersen, M., Izquierdo-Carrasco, F., Wappler, T., Rust, J., Aberer, A.J., Aspock, U., Aspock, H., Bartel, D., Blanke, A., Berger, S., Bohm, A., Buckley, T.R., Calcott, B., Chen, J., Friedrich, F., Fukui, M., Fujita, M., Greve, C., Grobe, P., Gu, S., Huang, Y., Jermiin, L.S., Kawahara, A.Y., Krogmann, L., Kubiak, M., Lanfear, R., Letsch, H., Li, Y., Li, Z., Li, J., Lu, H., Machida, R., Mashimo, Y., Kapli, P., McKenna, D.D., Meng, G., Nakagaki, Y., Navarrete-Heredia, J.L., Ott, M., Ou, Y., Pass, G., Podsiadlowski, L., Pohl, H., von Reumont, B.M., Schutte, K., Sekiya, K., Shimizu, S., Slipinski, A., Stamatakis, A., Song, W., Su, X., Szucsich, N.U., Tan, M., Tan, X., Tang, M., Tang, J., Timelthaler, G., Tomizuka, S., Trautwein, M., Tong, X., Uchifune, T., Walzl, M.G., Wiegmann, B.M., Wilbrandt, J., Wipfler, B., Wong, T.K., Wu, Q., Wu, G., Xie, Y., Yang, S., Yang, Q., Yeates, D.K., Yoshizawa, K., Zhang, Q., Zhang, R., Zhang, W., Zhang, Y., Zhao, J., Zhou, C., Zhou, L., Ziesmann, T., Zou, S., Li, Y., Xu, X., Zhang, Y., Yang, H., Wang, J., Wang, J., Kjer, K.M., Zhou, X., 2014. Phylogenomics resolves the timing and pattern of insect evolution. Science 346, 763–767.

Nagarkar-Jaiswal, S., DeLuca, S.Z., Lee, P.T., Lin, W.W., Pan, H., Zuo, Z., Lv, J., Spradling, A.C., Bellen, H.J., 2015. A genetic toolkit for tagging intronic MiMIC containing genes. eLife, 4.

Nie, J., Mahato, S., Mustill, W., Tipping, C., Bhattacharya, S.S., Zelhof, A.C., 2012. Cross species analysis of Prominin reveals a conserved cellular role in invertebrate and vertebrate photoreceptor cells. Dev. Biol. 371, 312–320.

Nie, J., Mahato, S., Zelhof, A.C., 2014. The actomyosin machinery is required for Drosophila retinal lumen formation. PLoS Genet. 10, e1004608.

Nie, J., Mahato, S., Zelhof, A.C., 2015. Imaging the Drosophila retina: zwitterionic buffers PIPES and HEPES induce morphological artifacts in tissue fixation. BMC Dev. Biol. 15, 10.

Osorio, D., 2007. Spam and the evolution of the fly's eye. Bioessays 29, 111–115.

Pellikka, M., Tanentzapf, G., Pinto, M., Smith, C., McGlade, C.J., Ready, D.F., Tepass, U., 2002. Crumbs, the Drosophila homologue of human CRB1/RP12, is essential for photoreceptor morphogenesis. Nature 416, 143–149.

Rodrigue, N., Lartillot, N., 2014. Site-heterogeneous mutation-selection models within the PhyloBayes-MPI package. Bioinformatics 30, 1020–1021.

Sauman, I., Briscoe, A.D., Zhu, H., Shi, D., Froy, O., Stalleicken, J., Yuan, Q., Casselman, A., Reppert, S.M., 2005. Connecting the navigational clock to sun compass input in monarch butterfly brain. Neuron 46, 457–467.

Stamatakis, A., 2014. RAxML version 8: a tool for phylogenetic analysis and post-analysis of large phylogenies. Bioinformatics 30, 1312–1313.

Stern, D.L., Orgogozo, V., 2008. The loci of evolution: how predictable is genetic evolution? Evolution 62, 2155–2177.
Voss, M., Schroder, B., Fluhrer, R., 2013. Mechanism, specificity, and physiology of signal peptide peptidase (SPP) and SPP-like proteases. Biochim. Biophys. Acta 1828, 2828–2839.
Wang, C.H., Hsu, S.J., 1982. The compound eye of the Diamondback moth, Plutella xylostella (L.) and its pigment migration. Bull. Inst. Zool. Acad. Sin. 21, 75–92.
Yu, M., Liu, Y., Li, J., Natale, B.N., Cao, S., Wang, D., Amack, J.D., Hu, H., 2016. Eyes shut homolog is required for maintaining the ciliary pocket and survival of photoreceptors in zebrafish. Biol. Open 5, 1662–1673.
Zelhof, A.C., Bao, H., Hardy, R.W., Razzaq, A., Zhang, B., Doe, C.Q., 2001. Drosophila Amphiphysin is implicated in protein localization and membrane morphogenesis but not in synaptic vesicle endocytosis. Development 128, 5005–5015.
Zelhof, A.C., Hardy, R.W., Becker, A., Zuker, C.S., 2006. Transforming the architecture of compound eyes. Nature 443, 696–699.